Functional Materials 16, No.3 (2009)

Radiation influence on characteristics of GaP light emitting diodes

A.Borzakovskyj, O.Gontaruk*, V.Kochkin, P.Litovchenko, V.Opilat, I.Petrenko, V.Tartachnyk

Institute for Nuclear Research, National Academy of Sciences of Ukraine,
47 Nauky Ave., 03028 Kyiv, Ukraine
*M.Dragomanov National Pedagogical University,
9 Pirogov St., Kyiv, Ukraine

Received March 6, 2009

The capacitance properties of GaP green and red LEDs have been studied. It was found the character of a doping impurity distribution in the depleted region and the junction depth dependence on bias voltage and impurity concentration in the low-doped part of the *p-n* junction have been established. The dependences of those quantities on the irradiation dose have been obtained (for $E = 1$ MeV electrons). In the case of alpha-particle bombardment (10^2–10^3 cm^{-1}), anomalous high carrier removal rate is explained by formation of disordered regions in irradiated samples.

Представлены результаты исследования емкостных характеристик фосфидо-галлиевых диодов зеленого и красного свечения. Выяснен характер распределения легирующих примесей в пределах обедненной области, зависимость ширины перехода от приложенного напряжения и концентрации примеси в слабо легированной части *p-n*-перехода. Определена зависимость этих величин от дозы облучения (для электронов с $E = 1$ МэВ). Аномально большое значение скорости удаления носителей при бомбардировании α-частицами (10^2–10^3 см$^{-1}$) объясняется образованием в облученных образцах областей разупорядочения.

GaP light emitting diodes (LEDs) are mostly used as visible light emitters [1–4]. The value of diode quantum yield, its operating stability, longevity and reliability are defined by the parameters of the grown *p-n* junction, which depend strongly on external factors, in particular, ionizing irradiation.

Although the radiation-induced changes in the diode base and structure defect properties were revealed earlier [5–15], the destructive radiation influence on main GaP device characteristics was studied not clear enough. In this work, presented are the study results of GaP *p-n* junction capacitance properties, the distribution of main doping impurities forming the electron-hole junction, and influence of electron and alpha-particle irradiation on the barrier capacity. We have considered the features of different radiation beams action and the dose dependences on radiative recombination intensity.

The light emitting diodes produced by double liquid epitaxy film growing on GaP substrate were used. Red light diodes were obtained by Te doping with concentration $8 \cdot 10^{17}$ cm^{-3} for *n*-region and by zinc and oxygen simultaneously for *p*-region. In order to decrease of the Auger recombination loss, the latter layer was doped to the charge carrier concentration of 10^{17} cm^{-3}. The layer thickness values were $d_n = 50$–60 μm, $d_p = 20$–30 μm, the sample area was 1 mm^2. For green diodes, *n*- and *p*-regions were doped by nitrogen and zinc, respectively, to corresponding concentrations $n =$

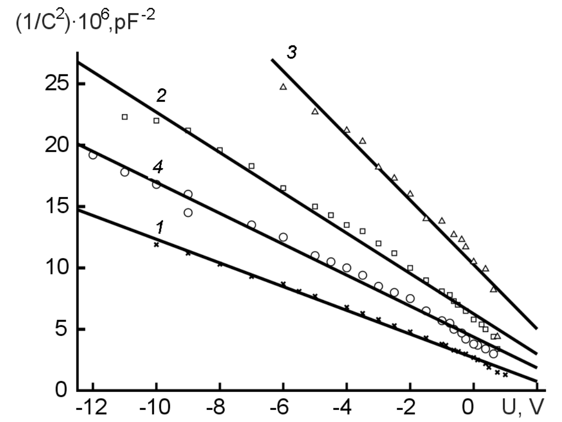

Fig. 1. Capacity-voltage characteristics of GaP red diodes, irradiation by 1 MeV electrons at 300 K. *1* — initial, *2* — irradiation $\Phi = 7.8\cdot10^{16}$ cm^{-2}, $N = 7.6\cdot10^{16}$ cm^{-3}, *3* — irradiation $\Phi = 2.4\cdot10^{17}$ cm^{-2}, $N = 4.63\cdot10^{16}$ cm^{-3}, *4* — calculated dependence.

10^{17} cm^{-3}, $p = 5\cdot10^{17}$ cm^{-3}, at the sample area 0.25 mm^2. The capacity-voltage characteristics were measured at 77 and 300 K. The samples were irradiated at $T = 300$ K by gamma-rays in a KU-6000 cobalt unit; by 1 MeV electrons using an ElT-1.5 accelerator and by 27.2 MeV α-particles, in a U-120 cyclotron. The gamma dose rate of Co^{60} was 500 rad/s. The electron beam was positioned to the diode p-side transversally to the p-n junction. As 1 MeV electron penetration depth in GaP is about 1 mm, defects were formed at a uniform density over the whole sample volume. An intense cooling with nitrogen vapor made it possible to decrease the exposure time (40 min for $\Phi = 1.2\cdot10^{17}$ cm^{-2}). The alpha beam density was 50 nA/cm^2 and water cooling was used.

In order to enhance the measurement accuracy, the equipment was calibrated after each irradiation by using a standard light emitting diode. Diodes with low-frequency brightness vibrations (several Hz) were eliminated from next experiments.

The value of barrier capacity of asymmetric sharp p-n junction is known to be determine as

$$C_b = S\sqrt{\frac{\varepsilon\varepsilon_0 qN}{2(U + U_k)}}, \qquad (1)$$

where S-is p-n junction area [16]; N, the ionized impurity concentration in low-doped region; U_k, the contact potential difference.

The $1/C^2$ dependences on reverse bias for initial (*1*) and irradiated (*2, 3*) red diode are given in Fig. 1. The linear $1/C^2(V)$ dependence testifies a sharp character of impurity distribution in the low-doped part of the junction. For comparison, the $1/C^2(V)$ dependence for asymmetric GaP p-n-junction is shown calculated using the expressions [16]

$$\frac{1}{C^2} = \frac{2L_D^2}{S\varepsilon_0\varepsilon}(\beta V_k \pm \beta V - 2), \qquad (2)$$

$$L_D = \sqrt{\frac{\varepsilon\varepsilon_0}{qN\beta}}; \quad \beta = \frac{q}{kT}. \qquad (3)$$

The Debye length and space charge region width calculated as a function of impurity concentration are shown in Fig. 2 (a, b). Parameters $L_D = 1,\ 2\cdot10^{-2}$ μm for $N = 10^{17}$ cm^{-3} and $V_k = 2.24$ V are used.

The electron irradiation ($\Phi_1 = 7.8\cdot10^{16}$ cm^{-2}, $\Phi_2 = 2.4\cdot10^{17}$ cm^{-2}) causes a sharp increase in the slope of $1/C^2(V)$ curves due to the reduction of the free carrier concentration resulting from compensating influence of deep radiation defect levels ($n_1 = 7.6\cdot10^{16}$ cm^{-3}, $n_2 = 4.63\cdot10^{16}$ cm^{-3}).

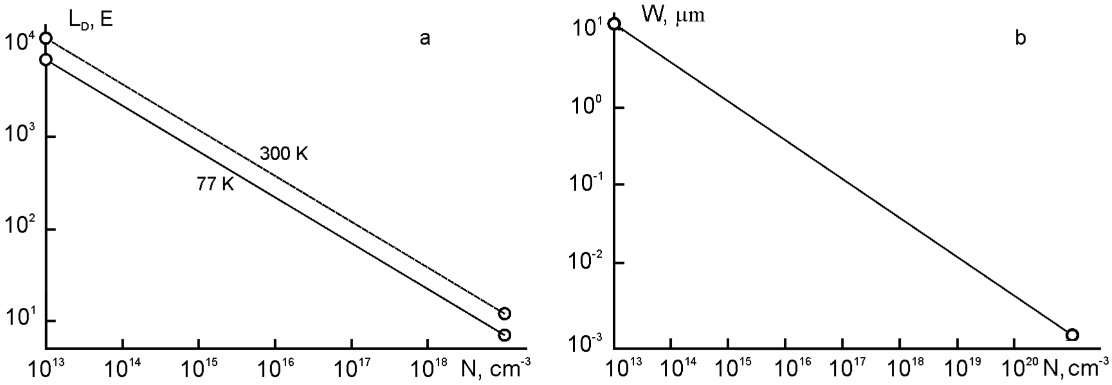

Fig. 2. Debay lenght L(a) and space charge region with (b) as a function of the impurity concentration.

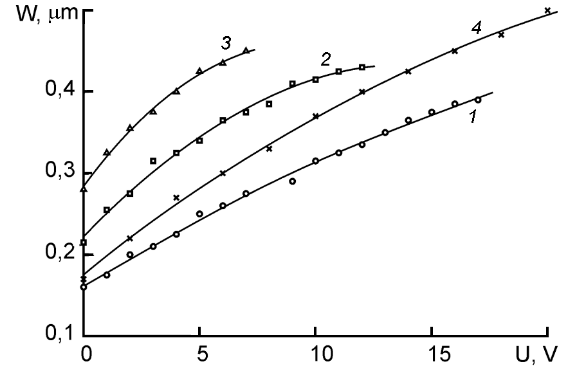

Fig. 3. Space charge width as a function of reverse bias for red GaP:ZnO,O diode. *1* — initial, *2* — irradiated, $\Phi = 7.8 \cdot 10^{16}$ cm^{-2}; *3* — irradiated, $\Phi = 2.4 \cdot 10^{17}$ cm^{-2}; *4* — calculated value.

The space charge region width depends on bias and ionized impurity concentration, which defines also the Debye length L_D

$$W = L_D\sqrt{2(\beta V_k - 2)}. \qquad (4)$$

Results of calculated $W(U_R)$ at $U_R = 0$ and experimental $W(U_R)$ obtained from $1/C^2(V)$ dependences (1, 2, 3 curves) for ionizing impurity concentration $N = 10^{17}$ cm^{-3} are given in Fig. 3. A satisfactory agreement of the both curves in the region of low bias (<3 V) is observed for the initial sample. At higher voltage, the difference between W_{theor} and $W_{exper.}$ occurs, because properties of a real diode are more complicated than the flat condenser model.

Electron irradiation ($\Phi = 2.4 \cdot 10^{17}$ cm^{-2}) leads to doubling of the space charge region width (at zero bias) and to the decrease of contact potential difference (Fig. 1); this is also caused by the compensating influence of radiation defects. A similar influence is observed in the case of gamma-rays of Co^{60}. It is seen in Fig. 4 that the maximum $1/C^2(V)$ slope changes occur at $\Phi_\gamma = 10^5$ rad. Then the curves nearly coincide even at $\Phi = 1.18 \cdot 10^6 \div 5 \cdot 10^7$ rad. Such effect is known as low-dose effect. For GaP, it was observed for the first time in [17]. The radiation-induced diffusion in crystals at high exitation levels is the most possible reason for that process [18]. Atoms occupying unstable positions in the lattice restore its equilibrium under the first irradiation and the subsequent dose increase causes no changes (Fig. 4).

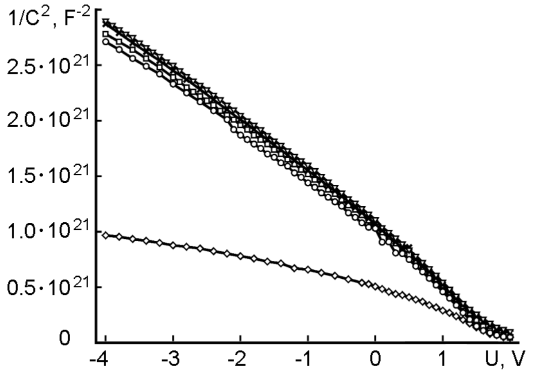

Fig. 4. $1/C^2$ dependence nn V for green diode; ◊ – initial, ○ – γ-rays, $\Phi = 10^5$ rad, □ — $\Phi = 1.18 \cdot 10^6$ rad, × – $\Phi = 10^7$ rad, ∇ – $\Phi = 5 \cdot 10^7$ rad.

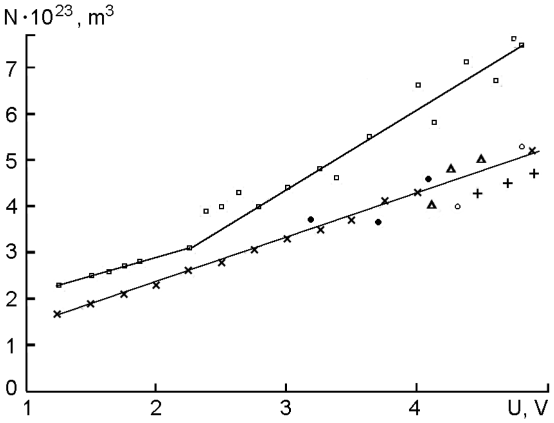

Fig. 5. Concentration dependences N_d on bias U in GaP green diodes at 300 K: □ — initial sample, Δ – $\Phi = 10^5$ rad, × – $\Phi = 1.18 \cdot 10^6$ rad, ○ – $\Phi = 5 \cdot 10^6$ rad, + – $\Phi = 10^7$ rad, ● – $\Phi = 5 \cdot 10^7$ rad.

The impurity concentration distribution in the low-doped part of the junction is described [19] as

$$N(x) = -\frac{C_b^3}{q\varepsilon\varepsilon_0 S^2}\left(\frac{dC_b}{dU}\right)^{-1}. \qquad (5)$$

This dependence for initial (*1*) sample and for those irradiated with different gamma-ray doses are shown in Fig. 5. It is seen that the sample become essentially homogeneous after first irradiation. The $N(U)$ curve shows also the existence of some concentration distribution gradient in green diodes.

Using the expression for the maximum junction field intensity

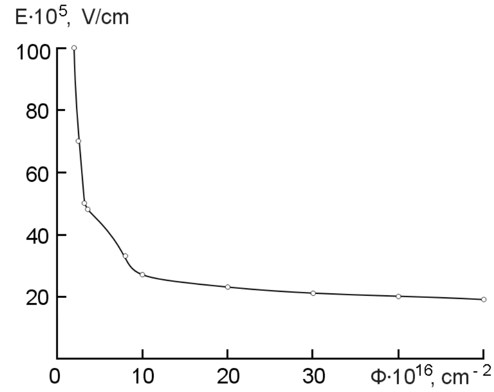

Fig. 6. Dose dependence of maximal electrical field intensity for GaP *p-n* junctions.

$$E_m(U) = \frac{Z(U + U_k)}{\varepsilon\varepsilon_0 S(Z - 1)} C_b(U) \qquad (6)$$

($Z = 2$ in our case) and the capacity dose dependence, it is possible to obtain the maximal junction field as a function of the integral particle fluence. It is seen in Fig. 6 that there is a maximum dose after which the field does not change essentially.

The radiation-induced defect concentration is

$$N_d = \sigma \cdot N_A \Phi, \qquad (7)$$

where σ is the defect cross-section; N_A, atomic concentration; Φ, the integral fluence.

The calculated electron interaction cross-section for different electron energies according to the McKinley-Feshbach model [20] is presented in Fig. 7.

The defect formation efficiency for γ-rays, 1 MeV electrons and 27.2 MeV α-particles can be compared by comparing the carrier removal rate. To that end, the γ irradiation (rad) is to be converted to phot/cm^2. For gamma-rays $E_\gamma = 1$ MeV, 1Gy = 10^2 rad = 1 J/kg and GaP density $\rho^{\mathrm{GaP}} = 4{\cdot}10^{13}$ g/cm^3. Then 1 rad = $6.25{\cdot}10^7$ photons.

The calculation results for all irradiation kinds are as follows :

$$\left(\frac{dn}{d\Phi}\right)_e = (1 \div 0.1)\mathrm{cm}^{-1};$$
$$\left(\frac{dn}{d\Phi}\right)_\gamma = (10 \div 15)\mathrm{cm}^{-1}; \qquad (8)$$
$$\left(\frac{dn}{d\Phi}\right)_{\alpha^{++}} = (10^2 \div 10^3)\mathrm{cm}^{-1}.$$

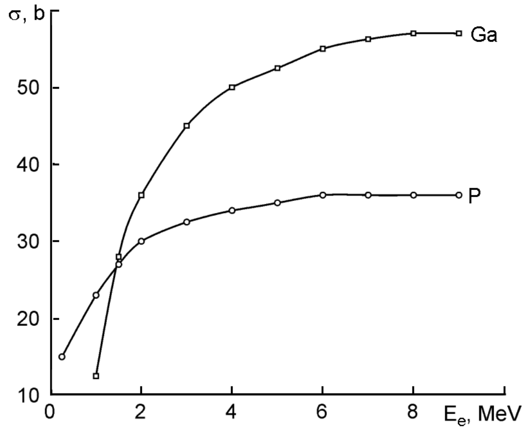

Fig. 7. Dependences of the defect creation cross section on electron energy in Ga and P sublattices.

The giant value of carrier removal rate for alpha-particles is like to be caused by the formation of disorder regions during irradiation. This fact correlates with results of capacity measurements as well as with emission characteristics of LEDs. At low fluences of alpha particles as compared to electron irradiation, the diode capacity becomes independent of bias and emitting recombination is zeroed.

If the mean cross-section of defect formation for 1 MeV electrons is believed to be 20 barn (Fig. 7), then the mean concentration of primary defects in GaP for electron fluence $\Phi = 7.8{\cdot}10^{16}$ cm^{-2} is

$$N^e_{def.} = 20 \cdot 10^{-24} \cdot 2.46 \cdot 10^{22} \cdot 7.8 \cdot 10^{16} = 3.84 \cdot 10^{16}\mathrm{cm}^{-3}. \qquad (9)$$

For both gamma- and alpha-irradiations, those values must differ in the same manner as their carrier removing rates:

$$N^\gamma_{def.} \approx 5 \cdot 10^{17}\mathrm{cm}^{-3}; \qquad (10)$$
$$N^{\alpha^{++}}_{def.} \approx (10^{18} \div 10^{19})\mathrm{cm}^{-3}.$$

Irradiation of GaP LEDs by electrons, gamma-rays and reactor neutrons results in a monotonous decrease of their emission intensity. As a rule, there no additional bands arise in the emission spectrum, but in some samples a sharp near-edge line ($h\nu = 2.311$ eV, 77 K) appears that is absent in initial samples. As such line does not exist at room temperature, it can be assumed to be of exciton origin. This center is formed most likely by radiation defect and uncontrollable impurity.

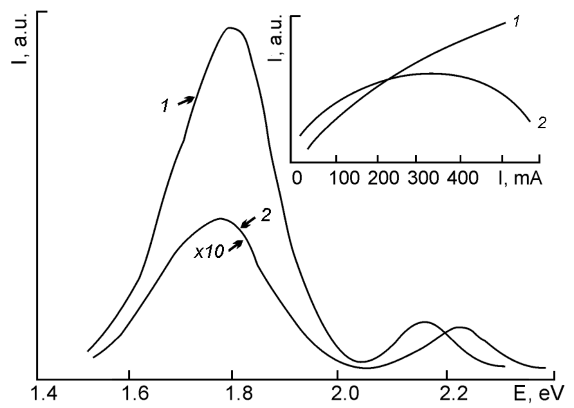

Fig. 8. GaP electroluminescence intensity spectra at 300 K: *1* — I = 20 mA, *2* — I = 800 mA. The insert-emitting intensity as a function of the *p-n*-current: *1* — green band, *2* — red band.

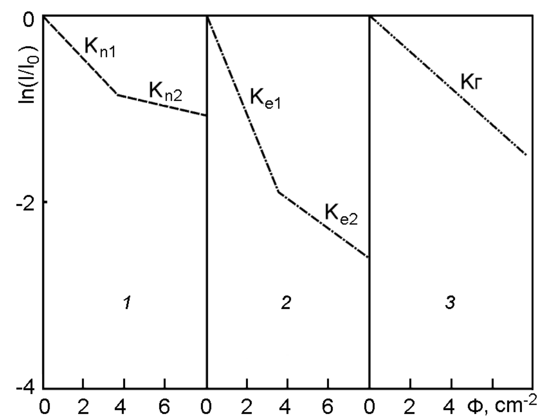

Fig. 9. Dose dependences of emitting intensities: *1* — neutrons, *2* — electrons, *3* — gamma rays.

The red band intensity ($h\nu = 1.8$ eV) dependence on the injection level for irradiated diode trends to saturation (see Fig. 8). This results obviously from the high radiation defect concentration, connected with radiationless levels in forbidden band of the semiconductor. Such recombination dominates in the irradiated sample, thus, the increase of excitation power leads to the increase of the radiationless events.

The dose dependences of diode brightness are shown in Fig. 9. It is seen that drop of emission intensities for all kinds of irradiation is well described by the exponential law

$$I = I_0 \exp(-K\Phi), \qquad (11)$$

where I_0, I – the emission intensity of initial and irradiated diodes; K, the brightness degradation coefficient, which characterizes the emission degradation. It is seen from the Figure that the degradation process for electron and neutron irradiation consists of two components. The fast degradation prevails at the initial irradiation stage. After attaining of a certain dose, it trends to slower changes. In the case of neutrons, the slowing-down of the degradation process starts earlier than for electrons. The difference is caused by the complex defects (disorder regions) arising in GaP LEDs due to neutrons. The fast component is defined by the simple point defects. Those appear in neutron irradiated samples, the gamma-irradiation of the reactor being their source. The influence of secondary defects (impurity complexes, point defect associations and divacancies, etc.) is manifested most probably at the second, low degradation stage. The ratio of degradation coefficients for reactor neutrons, 1 MeV and γ-quanta of Co^{60} is $K_{H1}{:}K_{e1}{:}K_1 = 10^4{:}10^2{:}1$. Thus, the complex defects, induced by neutrons are the most effective radiationless recombination centers.

To conclude, the epitaxial GaP LED's are characterized by a sharp impurity distribution within the low-doped region of *p-n* junction. The experimental *C*(*V*) curve is close to the calculated one. The volume charge region width depends linearly on the impurity concentration. Irradiation with 1 MeV electrons increases this width, this being a result of the compensating effect due to deep levels of radiation-induced defects. In diodes irradiated by gamma-rays, the low dose effect is observed, caused by the radiation-induced activation of non equilibrium structure defects. High ionizing levels of lattice atoms are governing in the process. A low gradient of impurity distribution is observed in green LEDs. The irradiation equalizes partly the inhomogeneous carrier distribution $N(x)$. It has been also revealed that the *p-n* junction field E decreases monotonously under irradiation and at large electron fluences ($\Phi = 5\cdot10^{16}$ cm^{-2}) E becomes independent of Φ. The large value of the carrier removal rate in samples irradiated by alpha-particles is probably caused by the appearing of disorder regions. The drop of emission intensity during diode irradiation is a result of deep nonradiative levels creation in GaP forbidden zone. The degradation coefficients for all irradiation kinds have been found. It appears that degradation coefficient is four orders higher for neutrons than those for gamma-rays of Co^{60} due to the formation of disorder regions during neutron irradiation.

References

1. A.Berg, P.Dean, Light Emitting-Diodes, Mir, Moskow, 1979 [in Russian].
2. V.A.Brzezinski, M.V.Shevchenko, Optoelectronics, ISD, Kyiv (1995) [in Ukrainian].
3. S.Nikiforov, *Componenty i Technologii*, **7**, 170 (2007).
4. I.Prochaska, K.I.Hamal, B.Sopko et al., *Nucl. Inst. and Meth. Phys. Res. A*, 437 (2006).
5. T.Endo, T.Nichimura, K.Nakakuki et al., *Jap. J. Appl. Phys.*, **11**, 2107 (1998).
6. T.Endo, J.Hirosaki, E.Ushida et al., *Jap. J. Appl. Phys.*, **28**, 1864 (1989).
7. L.Dlubek, R.Krause, W.Hoppe, Untersuchunger von Kristallbsunfehlern in Metallen and Haibleitern mit Positronen-Beitrag, Martin-Luter-Universitaet, Wittenberg (1986).
8. V.N.Brudnyi, S.N.Grinyaev, V.D.Kuznetsova, *Fizika i Tekhn. Polupr.*, **37**, 557 (2003).
9. K-H.Heckner, G.Majoros, A.Kraft et al., *Phys. Stat. Sol.(a)*, **148**, 407 (2006).
10. I.A.Bocharova, S.A.Malyshev, *Zh. Prikl. Spektr.*, **73**, 78 (2006).
11. T.Tanno, K.Suto, Y.Ouata et al., *Materials Science in Semiconductor Proceeding*, 441 (2003).
12. A.E.Belyaev, N.S.Boltovets, V.N.Ivanov, *Fizika i Tekhn. Polupr.*, **42**, 463 (2008).
13. I.I.Patskun, L.M.Markovich, *Fiz. i Khim. Tverd. Tila*, **5**, 738 (2004).
14. Z.Bichong, F.Yangling, H.Yinghao, *Phys. Stat. Sol. A*, **102**, 533 (1987).
15. F.Domeniquez-Adame, J.Piqueras, de-Diago et al., *Solid State Commun.*, **6**, 665 (1988).
16. S.Sze, Physics of Semiconductor Devices, Mir, Moskow, 1984 [in Russian].
17. V.Tartachnyk, I.Petrenko, P.Litovchenko, *Fiz. Khim. Tverdogo Tila*, **4**, 474 (2003).
18. V.S.Vavilov, A.E.Kiv, O.R.Niyazova, Mechanisms of Formation and Migration of Defects in Semiconductors, Nauka, Moscow (1981) [in Russian].
19. L.S.Berman, Capacitive Methods of Semiconductor Research, Nauka, Leningrad (1972) [in Russian].
20. W.McKinley, H.Feshbach, *Phys. Rev.*, **74**, 1759 (1948).

Вплив радіації на характеристики фосфідо-галієвих світлодіодів

А.Е.Борзаковський, О.М.Гонтарук, В.І.Кочкін, П.Г.Литовченко, В.Я.Опилат, І.В.Петренко, В.П.Тартачник

Наведено результати дослідження ємнісних характеристик зелених та червоних фосфідо-галієвих діодів. Визначено характер розподілу легуючих домішок у межах збідненої області, залежність ширини переходу від прикладеної напруги та концентрації домішки у слаболегованій частині p-n-переходу. Одержано залежність цих величин від дози опромінення (для електронів з $E = 1$ МеВ). Аномально велике значення швидкості видалення носіїв при бомбардуванні α-частинками (10^2–10^3 см$^{-1}$) пояснюється формуванням в опромінених зразках областей розупорядкування.